Ion implantation of boric molecules for silicon solar cells

Jan Krügener [a,*], Robby Peibst [b], Eberhard Bugiel [a], Dominic Tetzlaff [a], Fabian Kiefer [b],
Marcel Jestremski [a], Rolf Brendel [b,c], H. Jörg Osten [a,c]

[a] Institute of Electronic Materials and Devices (MBE), Leibniz Universität Hannover, Schneiderberg 32, D-30167 Hannover, Germany
[b] Institute for Solar Energy Research Hamelin (ISFH), Am Ohrberg 1, D-31860 Emmerthal, Germany
[c] Laboratory of Nano and Quantum Engineering (LNQE), Leibniz Universität Hannover, Schneiderberg 39, D-30167 Hannover, Germany

ARTICLE INFO

ABSTRACT

We investigate the electrical and structural characteristics after ion implantation of BF$_x$ ($x = 1,2$) for silicon solar cells. Compared to non-amorphizing species, e.g. B, amorphizing species, like BF$_x$, offer the possibility to lower the thermal budget, which is needed for the curing of implant-induced crystal defects. For implant energies above 30 keV (BF$_2$) we find a strong degradation of the charge carrier lifetime in the volume as well as an increase of the emitter saturation current density J_0 compared to implantation of elemental boron. This behavior can be related to a defective solid phase epitaxy during the recrystallization in the annealing process after implantation. Implantation of BF$_2$ at 10 keV and subsequent annealing at 1050 °C for 30 min results in J_0 values of 41 ± 3 fA/cm² for a planar, Al$_2$O$_3$ passivated 133 Ω/sq emitter. Furthermore, using implantation of BF$_2$ at 20 keV allows lowering the annealing temperature from 1050 °C, as commonly used for elemental boron, to 950 °C. The latter results in a J_0 of 58 ± 2 fA/cm² for a planar, Al$_2$O$_3$ passivated 141 Ω/sq emitter.

© 2015 Elsevier B.V. All rights reserved.

1. Introduction

Ion implantation of boron offers the possibility of single-sided (or even patterned) high-quality emitter formation for n-type silicon solar cells [1]. After implantation a high temperature annealing step is required to electrically activate the implanted ions and to cure the implant-induced crystal defects (e.g. [2]). The dissolution of these defects (like dislocation loops [3] or boron interstitial clusters [4,5]) requires either a high temperature step (several 10 min above 1000 °C) after implantation (e.g. [6]) or an etch-back step of the emitter surface after annealing at lower temperatures [7].

After implantation of higher mass ions (like phosphorous) and subsequent annealing around 900 °C no crystal defects were observed [8]. This behavior is associated with an amorphization of the near surface region during implantation and the recrystallization process via solid phase epitaxy (SPE) during subsequent annealing. In microelectronic technology, BF$_2$ (mass 49) is often used instead of B (mass 11), not only to achieve an amorphization of the surface region but also to prepare very shallow implant profiles. Literature reports the impact of the fluorine on the sheet resistance (R_{sheet}) [9] and on the electrical activation of boron [10].

The diffusion of boron in the presence of fluorine is another well-studied topic [11]. Unfortunately, the impact of BF$_2$ and in particular the impact of the fluorine, on the electrical properties important for solar cells (emitter saturation current densities J_0, minority carrier lifetime τ) has not been reported in the literature so far.

The technology to transfer ion implantation into photovoltaic industry will be most likely based on Plasma Immersion Ion Implantation (PIII) [12]. In that case, the whole spectrum of ion species present in the plasma of the ion source will be implanted. That means that for boron implants, where typically BF$_3$ is used as precursor, a large amount of fluorine is implanted in addition to the elemental boron.

2. Sample preparation

We use Czochralski-grown 3 Ω cm n-type Si(100) substrates (156 × 156 mm², pseudo-square) with an as-cut thickness of 180 μm. Prior to ion implantation, the wafers are saw damage-etched and RCA cleaned. We prepare two kinds of samples: (a) samples with planar surfaces and (b) samples with anisotropic KOH-etched (textured) surfaces. The planar samples are used to characterize the impact of the basic implant parameters (ion energy, ion dose and implant angle) on J_0 and τ_{eff} after

* Corresponding author. Tel.: +49 511 762 4216; fax: +49 511 762 4229.
E-mail address: kruegener@mbe.uni-hannover.de (J. Krügener).

implantation of BF_2 and subsequent annealing. Here, BF_2 is used since it is known to provide the lion's share in BF_3 plasmas [13,14] and should therefore provide a suitable figure of merit for the evaluation of PIII of boron from BF_3.

The textured set of samples is used for BF_x implants on solar cell-like surfaces. Here BF and BF_2 are implanted with a dose of 2.5×10^{15} cm^{-2} with energies of 30 keV and 50 keV, respectively. Ion implantation of molecules leads to similar projected ranges for all of the atomic species within the molecules (e.g. as observed in SIMS [9]). The reason for this is an immediate dissociation of the molecules and splitting of the energy according to the mass fraction of the single species [15]. For example implantation of BF_2 at 50 keV leads to effective ion energies of 11 keV ($=[m_B/m_{BF2}] \times E_{implant}=E_B$) for B and 19 keV ($=[m_F/m_{BF2}] \times E_{implant}=E_F$) for F. The resulting projected ranges of the implanted B and F ions are 43.7 nm for BF (30 keV) as well as for BF_2 (50 keV), as determined by the TRIM code [16]. Additionally a reference sample implanted with elemental boron is prepared (2.5×10^{15} cm^{-2}, 10 keV, projected range 40 nm).

During ion implantation (VIISta HCS from Varian) the substrates are tilted by 6° towards ⟨100⟩. Subsequent defect annealing is performed in a conventional quartz furnace under inert ambient (dry N_2) at 1050 °C for 80 min (textured samples with BF_x and for B reference, plateau time), at 1050 °C for 20 min (section 3.2) or at 800–1050 °C for 30 min (Section 3.3). After ion implantation of elemental boron, annealing at 1050 °C for several 10 min leads to excellent emitter saturation current densities which are not affected by implant-induced crystal defects anymore [17,18]. The lower temperatures are used to evaluate the potential of reducing the thermal budget after BF_x, especially for BF_2 implantation.

The annealed samples are passivated on both sides by 10 nm Al_2O_3 deposited by atomic layer deposition plus a subsequent forming gas treatment at 350 °C for 10 min. τ_{eff} is measured by quasi-steady-state photo conductance method (QSSPC) using a Sinton Instruments WCT-120 setup. From the τ_{eff} measurements J_0 is extracted using the method of Kane and Swanson [19]. Structural investigations are performed with transmission electron microscopy (TEM, G2 F20 TMP from Tecnai) for the as-implanted and the annealed state.

With SENTAURUS Process [20] we simulate the resulting dopant distribution after ion implantation and subsequent annealing. From simulated doping profiles we calculate theoretical J_0 values with SENTAURUS Device [21], intentionally omitting any influence of a residual defect distribution. From the comparison of these defect-free J_0 values (assuming an Al_2O_3 surface passivation), we can determine the influence of implant-induced defects on J_0.

3. Results and discussion

3.1. Reference implantation of BF_x

In the first set of experiments we prepare 3 double-sided p^+np^+ samples on textured wafers: a reference sample and one sample with BF and BF_2, respectively. For the reference sample elemental boron is implanted at 10 keV with a dose of 2.5×10^{15} cm^{-2}. Subsequently, the sample is annealed at 1050 °C for 80 min since these annealing parameters are known to result in excellent emitter properties [18]. The corresponding measured inverse lifetimes as a function of the minority carrier density are given in Fig. 1. Applying the method of Kane and Swanson [19] on the sample implanted with elemental boron, we extract a J_0 of 60 ± 3 fA/cm² for a sheet resistance (R_{sheet}) of 58 Ω/sq.

Based on the reference sample, we implant 2 BF_x samples with the same dose (2.5×10^{15} cm^{-2}) for BF and BF_2 with energies of 30 keV and 50 keV, respectively. After implantation, the samples
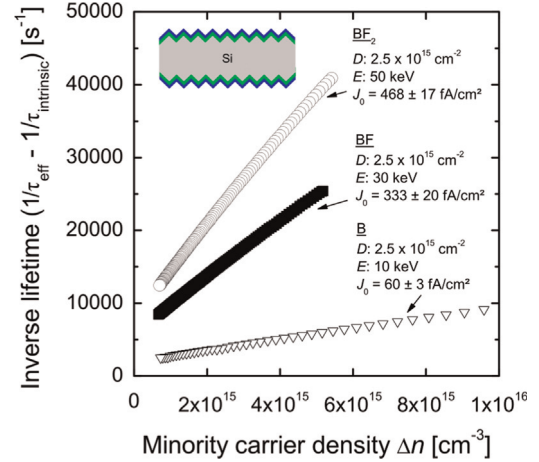

Fig. 1. Inverse lifetime as a function of the excess minority carrier density Δn after ion implantation of B, BF and BF_2 and subsequent annealing at 1050 °C for 80 min. The different ion energies are chosen in order to ensure comparable projected ranges for boron. J_0 is extracted from the slope at a minority carrier density of 5×10^{15} cm^{-3}.

are annealed at 1050 °C for 80 min. The corresponding measured inverse lifetimes as a function of the excess minority carrier density Δn after annealing are summarized in Fig. 1. Compared to the reference sample we find a much higher J_0 of 333 ± 20 fA/cm² for BF and 468 ± 17 fA/cm² for BF_2. At the same time, R_{sheet} increases to 99 Ω/sq for BF and 158 Ω/sq for BF_2. The higher R_{sheet} of the BF_x implanted samples compared to samples implanted with elemental B are associated with a decreased activation of B in the presence of F [9].

These high J_0 values can originate from a different defect structure after annealing compared to elemental boron. For elemental boron, where due to technological reasons doses below the amorphization threshold are commonly used, the dominant defect species is determined by the annealing temperature and the used ion dose [22]. At temperatures of 1050 °C as used here, commonly dislocation loops are observed [17].

In order to clarify the origin of the high J_0 after BF_x implantation, we perform structural TEM investigations in the as-implanted and the annealed state. For the latter, we used the same samples which are already characterized by QSSPC as discussed above. The as-implanted state samples are prepared the same way but omitting the annealing step: implantation of 2.5×10^{15} cm^{-2} at 30 keV and 50 keV for BF and BF_2, respectively.

The results of the TEM investigations are shown in Fig. 2. The as-implanted states of textured samples (see Fig. 2(a) and (c)) show a very similar structure for both implant species (BF and BF_2). At the surface, we find the expected amorphous region as a result of the ion bombardment. The layer thickness is not homogeneous across the sample surface due to the tilt angle during implant, (for more details see discussion in Ref. [23]). Due to the tilt of 6° towards ⟨100⟩ during implantation, 2 sides of the texture pyramids are tilted into the ion beam and 2 sides are tilted out of the ion beam [23]. The thickness of the amorphous layer is around 23 nm for those pyramid sides tilted out of the ion beam, 30 nm for those sides tilted into the beam and 37 nm within the valleys in between the pyramids. Below this amorphous layer a highly defective but still crystalline layer can be resolved. The visible defect structure is caused by the agglomeration of point defects [24] whereas their density is not sufficient to result in an amorphization of the crystal. The samples implanted with BF_2 seem to be more damaged than those for BF. Nevertheless, a quantitative analysis is difficult from these images.